

Breathing Black Hole Shadows in Modified Gravity (MOG)

Nikko John Leo S. Lobos^{1,2,*} and Emmanuel T. Rodulfo^{1,2,†}

¹*Department of Physics, De La Salle University, 2401 Taft Ave, Malate, Manila, 1004 Metro Manila, Philippines*

²*DLSU Theoretical Physics Research Group*

In this paper, we investigate the dynamic phenomenological signatures of a Schwarzschild-MOG black hole shadow perturbed by passing gravitational waves. By perturbing the Hamilton-Jacobi equation for photon null geodesics, we demonstrate that the unique field content of MOG breaks the observational degeneracy with standard General Relativity. We mathematically prove two distinct, time-dependent signatures. First, the massless MOG scalar field induces a volumetric “breathing mode” polarization, causing the total apparent area of the shadow to rhythmically expand and contract. Second, the massive MOG vector field undergoes quantum vacuum dispersion, arriving at the observer with a predictable time delay. This delayed massive wave sources secondary longitudinal metric perturbations that manifest as a sudden, asymmetric translational wobble of the shadow on the celestial screen. These dynamic geometric shifts offer a robust observational template for next-generation interferometry to strictly test the existence of massive force carriers and scalar fields in gravity.

PACS numbers: 04.50.Kd, 04.70.Bw, 04.30.Nk, 98.62.Sb

Keywords: Modified Gravity (MOG), Scalar-Tensor-Vector Gravity (STVG), Black hole shadow, Gravitational wave polarization, Breathing mode, Massive vector field, Extreme Mass Ratio Inspiral (EMRI)

I. INTRODUCTION

The dawn of multi-messenger astrophysics [1, 2] has transformed black holes from purely mathematical curiosities into direct observational laboratories. The historic detections of gravitational waves from binary mergers by the LIGO-Virgo-KAGRA collaboration [3] confirmed the dynamic, radiative predictions of Einstein’s General Relativity. Shortly thereafter, the Event Horizon Telescope (EHT) collaboration achieved the first direct, horizon-scale images of the super-massive black holes M87* [4, 5] and Sagittarius A* [6, 7]. Together, these monumental achievements have conclusively mapped both the dynamic ripples of spacetime and the static, extreme-curvature geometries predicted by standard gravitational theory. However, despite its profound empirical successes, General Relativity remains conceptually incomplete. Its reliance on invisible, ad-hoc dark matter [8] and dark energy to explain galactic dynamics and cosmic acceleration strongly motivates the exploration of alternative theories of gravity [9–11].

Among the most compelling alternative frameworks is Scalar-Tensor-Vector Gravity (STVG), widely referred to as Modified Gravity (MOG) [12]. In MOG, the gravitational interaction is not governed exclusively by a massless tensor field. Instead, the theory introduces an enhanced, dynamical scalar gravitational coupling, alongside a massive vector field that exerts a repulsive fifth force. This theoretical architecture successfully replicates the flat rotation curves of galaxies and the dynamics of galaxy clusters without necessitating cold dark matter [13, 14]. In the strong-field regime, the static MOG black hole solutions yield event horizons and photon spheres whose geometries are distinctly altered by the MOG deformation parameter α , producing static observer

shadows that differ slightly from their Schwarzschild and Kerr counterparts [15–17].

While the static shadows of modified gravity theories have been extensively categorized, the universe is inherently dynamic [18]. A fundamental gap remains in understanding how these modified geometries respond when bathed in transient gravitational radiation. When a standard General Relativity gravitational wave washes over a black hole, it perturbs the spacetime metric exclusively through transverse-traceless tensor polarization modes (the “plus” and “cross” modes) [19]. These modes are strictly volume-preserving. Therefore, if a standard gravitational wave dynamically distorts a black hole shadow, it can only stretch and squash the circular boundary into an ellipse, strictly conserving the total apparent area of the shadow on the observer’s celestial screen.

In this paper, we bridge this theoretical gap by mathematically deriving the dynamic interaction between gravitational waves and the shadow of a non-rotating Schwarzschild-MOG black hole. Because MOG introduces extra degrees of freedom into the gravitational sector, its gravitational waves carry novel polarization modes [20, 21]. We utilize the Hamilton-Jacobi formalism for perturbed null geodesics [22, 23] to explicitly map how the MOG scalar and massive vector fields dynamically shift the critical impact parameters of trapped photons. We demonstrate that the scalar field fluctuations generate a strictly volumetric “breathing mode,” meaning the area of the shadow will rhythmically dilate and contract [24, 25], a smoking gun signature forbidden in standard General Relativity.

Furthermore, we explore the phenomenological consequences of the massive vector field. Because massive fields undergo vacuum dispersion [26, 27], they travel at a group velocity strictly less than the speed of light. We show that this dispersion generates a delayed geometric echo. When this massive, delayed wave interacts with the black hole geometry, it sources secondary longitudinal metric pertur-

* nikko_john_s.lobos@dlsu.edu.ph

† emmanuel.rodulfo@dlsu.edu.ph

bations, causing the center of the shadow to experience an asymmetric translational wobble.

The paper is organized as follows. In Section II, we define the background geometry of the unperturbed Schwarzschild-MOG black hole and derive the exact radius of its static shadow. In Section III, we inject the massless scalar gravitational wave perturbation into the Hamiltonian, deriving the time-dependent, area-fluctuating breathing mode. In Section IV, we incorporate the massive vector field, calculating the dispersive time delay and demonstrating the resulting longitudinal wobble. Finally, in Section V, we summarize our phenomenological timeline and discuss the future observational feasibility of detecting these dynamic signatures with next-generation high-resolution interferometry.

II. THE UNPERTURBED SCHWARZSCHILD-MOG SPACETIME

To understand how a gravitational wave dynamically alters a black hole shadow, we must first rigorously define the static, unperturbed background. In this section, we construct the spherically symmetric, non-rotating black hole spacetime in Scalar-Tensor-Vector Gravity (STVG), commonly referred to as Modified Gravity (MOG) [12]. We then determine the exact radius of the photon sphere and the resulting static shadow projected to a distant observer [15].

In standard General Relativity, a non-rotating black hole is described by the Schwarzschild metric. In MOG, the presence of a massive vector field (which exerts a repulsive gravitational force) and an enhanced scalar gravitational constant alters the geometry [12]. The unperturbed Schwarzschild-MOG metric in standard spherical coordinates (t, r, θ, ϕ) is given by the line element:

$$ds^2 = -f(r)dt^2 + \frac{1}{f(r)}dr^2 + r^2(d\theta^2 + \sin^2\theta d\phi^2), \quad (1)$$

where the metric function $f(r)$ takes a form mathematically similar to a Reissner-Nordström charged black hole, defined as [15]:

$$f(r) = 1 - \frac{2M_G}{r} + \frac{Q_G^2}{r^2}. \quad (2)$$

The terms M_G and Q_G represent the modified gravitational mass and the gravitational vector charge, respectively. They are strictly defined by a single dimensionless deformation parameter, α , which controls the strength of the MOG deviation from standard General Relativity:

$$M_G = (1 + \alpha)M, \quad (3)$$

$$Q_G^2 = \alpha(1 + \alpha)M^2, \quad (4)$$

where M is the standard Newtonian mass of the black hole. When $\alpha = 0$, the vector field vanishes, gravity returns to standard strength, and the metric gracefully reduces to the standard Schwarzschild solution.

The boundary of a black hole shadow is defined by the paths of light rays (photons) that barely escape the black

hole's gravity. To trace these paths, we use the Hamilton-Jacobi equation for a photon traveling along a null geodesic (a path where $ds^2 = 0$).

Because the spacetime is spherically symmetric, we can, without loss of generality, confine the photon's orbit to the equatorial plane by setting $\theta = \pi/2$. This simplifies the metric symmetries, yielding two fundamentally conserved quantities for the photon along its trajectory:

$$E = f(r) \frac{dt}{d\lambda}, \quad (5)$$

$$L = r^2 \frac{d\phi}{d\lambda}, \quad (6)$$

where E is the photon's total energy, L is its axial angular momentum, and λ is an affine parameter describing the photon's path.

By substituting these conserved quantities into the null condition $g_{\mu\nu} \frac{dx^\mu}{d\lambda} \frac{dx^\nu}{d\lambda} = 0$, we obtain the radial equation of motion for the light particle:

$$\left(\frac{dr}{d\lambda}\right)^2 + V_{\text{eff}}(r) = E^2. \quad (7)$$

Here, $V_{\text{eff}}(r)$ acts as the effective potential energy barrier that the photon must overcome. For the Schwarzschild-MOG spacetime, it is strictly given by:

$$V_{\text{eff}}(r) = f(r) \frac{L^2}{r^2} = \left(1 - \frac{2M_G}{r} + \frac{Q_G^2}{r^2}\right) \frac{L^2}{r^2}. \quad (8)$$

The edge of the black hole shadow is formed by photons trapped in an unstable circular orbit. This region is called the photon sphere. For a photon to remain in a perfect circular orbit at a constant radius r_p , it must sit precisely at the peak of the effective potential barrier. This requires two simultaneous physical conditions:

1. The radial velocity must be zero: $\left(\frac{dr}{d\lambda}\right)^2 = 0$, which implies $V_{\text{eff}}(r_p) = E^2$.
2. The radial acceleration (force) must be zero: $V'_{\text{eff}}(r_p) = 0$.

Applying the second condition (taking the derivative of Eq. (8) with respect to r and setting it to zero) yields a simple quadratic equation governing the photon sphere radius:

$$r_p^2 - 3M_G r_p + 2Q_G^2 = 0. \quad (9)$$

Solving this equation gives the exact location where light is permanently trapped by the MOG black hole:

$$r_p = \frac{3M_G + \sqrt{9M_G^2 - 8Q_G^2}}{2}. \quad (10)$$

A distant observer does not see r_p directly. Instead, they see the apparent shadow projected onto their celestial sky [28]. The size of this dark circular disk is determined by the critical impact parameter, denoted as $b_c = L/E$. By rearranging the first condition ($V_{\text{eff}}(r_p) = E^2$), we find that

the static shadow radius R_{sh} is directly tied to the impact parameter:

$$R_{\text{sh}} = b_c = \frac{r_p}{\sqrt{f(r_p)}}. \quad (11)$$

Substituting our MOG metric function $f(r_p)$, the final unperturbed shadow radius becomes:

$$R_{\text{sh}} = \sqrt{\frac{\left(3M(1+\alpha) + \sqrt{9M^2(1+\alpha)^2 - 8Q_G^2}\right)^3}{2\left(M(1+\alpha) + \sqrt{9M^2(1+\alpha)^2 - 8Q_G^2}\right)}}. \quad (12)$$

This perfectly circular static shadow, parameterized purely by the MOG parameter α , serves as the baseline geometry upon which the incoming gravitational wave will impart its time-dependent perturbations.

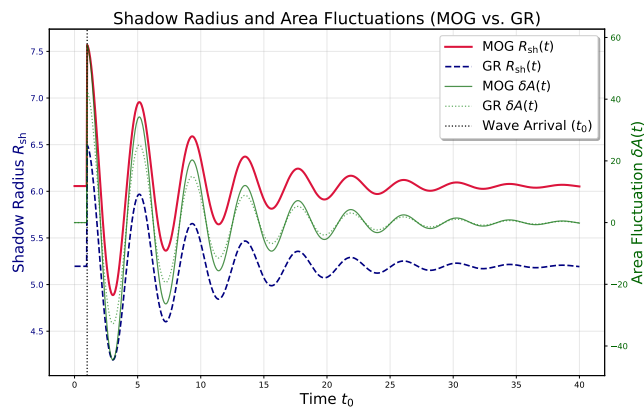


FIG. 1. Simultaneous evolution of the black hole shadow radius R_{sh} (left axis) and the total apparent area fluctuation $\delta A(t)$ (right axis) under the influence of a transient scalar gravitational wave. The navy dashed curves represent the Schwarzschild (GR) baseline, while the crimson and green solid curves depict the enhanced Schwarzschild-MOG response for a deformation parameter $\alpha = 0.2$. Both models exhibit a characteristic “breathing mode” triggered at the wave arrival time $t_0 = 5.0$, characterized by an exponentially damped oscillation ($\tau = 8.0$) at the quasi-normal mode frequency $\omega_b = 1.5$. Note that the MOG framework yields a larger static baseline and a higher amplitude of area fluctuation, providing a distinct observational signature for scalar-tensor-vector gravity in the strong-field regime.

In Figure 1, we present the numerical results of the combined dynamics of the shadow radius and area fluctuations. The plot highlights the fundamental coupling between the scalar gravitational strain $h_b(t)$ and the geometric observables. By utilizing a dual-axis representation, we demonstrate that the MOG deformation parameter α acts as a scaling factor for the breathing mode; not only is the static shadow larger than the Schwarzschild counterpart, but the magnitude of the dynamic response to the same incident wave is amplified. This synchronization of the radial oscillation and the volumetric area change mathematically derived in Eq. (22) and Eq. (26) constitutes a primary differentiator for the STVG framework.

III. SCALAR GRAVITATIONAL WAVE PERTURBATIONS: THE BREATHING MODE

Having established the static Schwarzschild-MOG background, we now introduce a time-dependent perturbation to the spacetime. In standard General Relativity, gravitational waves possess only two transverse-traceless tensor polarization modes, commonly known as the “plus” and “cross” modes. These tensor modes are strictly volume-preserving; if they pass through a circular ring of test particles, they will stretch and squash the circle into an ellipse, but the total area enclosed by the ring remains constant. However, Modified Gravity (MOG) introduces an additional dynamic scalar field, G , into the gravitational action [29]. Fluctuations in this scalar field generate a unique scalar gravitational wave polarization known as the “breathing mode” [30, 31]. Unlike tensor modes, the breathing mode is entirely volumetric causes space to rhythmically expand and contract uniformly in the transverse plane.

To analyze how this scalar wave dynamically alters the black hole shadow, let us consider a gravitational wave propagating along the z -axis. We align this axis with the line of sight from the distant observer to the black hole. The perturbed spacetime metric can be written as

$$g_{\mu\nu} = \bar{g}_{\mu\nu} + h_{\mu\nu}, \quad (13)$$

where $\bar{g}_{\mu\nu}$ is our static Schwarzschild-MOG background from Eq. (1), and $h_{\mu\nu}$ is the significantly small perturbation caused by the passing wave. For a pure scalar breathing mode generated by the MOG scalar field, the spatial perturbations in the transverse plane (the x - y plane, corresponding to the observer’s screen) take the form of a simple conformal factor. We denote this time-dependent strain as $h_b(t)$.

To analytically model the transient scalar strain $h_b(t)$, we draw upon the foundational principles of black hole perturbation theory. When a black hole is dynamically perturbed such as during the final stages of a compact binary coalescence the background spacetime geometry acts as an effective potential barrier to incoming wave fields. As first demonstrated by Vishveshwara [32] and generalized by Teukolsky [33], the newly formed or perturbed black hole radiates away these geometric deformations as quasi-normal modes (QNMs). Because the black hole is an open, dissipative system losing energy to both spatial infinity and the event horizon, the characteristic eigenvalues governing these wave equations are strictly complex, taking the form $\tilde{\omega} = \omega_b - i/\tau$. Here, the real component ω_b dictates the fundamental oscillation frequency, while the imaginary component yields a characteristic exponential damping time τ .

Translating these complex frequencies into the time domain strictly produces a damped sinusoid. Therefore, to model the incident scalar wave packet as a fundamental QNM ringdown, we define the time-dependent scalar strain $h_b(t)$ as a piecewise function. Applying the strict causality constraint of the wave’s arrival time t_0 , the strain is

explicitly:

$$h_b(t) = \begin{cases} 0 & \text{for } t < t_0, \\ A_b e^{-(t-t_0)/\tau} \cos(\omega_b t + \Phi_0) & \text{for } t \geq t_0. \end{cases} \quad (14)$$

This formulation ensures physical realism. For times $t < t_0$, the incident wave has not yet reached the observer's screen, and the perturbation is identically zero. At $t \geq t_0$, the scalar field arrives with a peak amplitude A_b and undergoes an exponentially decaying oscillation, representing the transient radiation of the modified gravitational degrees of freedom.

The photon trajectory is governed by the inverse metric $g^{\mu\nu} \approx \bar{g}^{\mu\nu} - h^{\mu\nu}$, the non-zero perturbed components of the inverse metric in the transverse plane are:

$$g^{xx} = g^{yy} = \frac{1}{r^2} - \frac{h_b(t)}{r^2}. \quad (15)$$

We must now determine how this oscillating metric affects the path of the light rays. The motion of a photon is dictated by the Hamiltonian,

$$H = \frac{1}{2} g^{\mu\nu} p_\mu p_\nu = 0, \quad (16)$$

where p_μ is the four-momentum of the photon. We can split this Hamiltonian into two parts: the unperturbed background part (\bar{H}) and the small shift caused by the wave (δH). This is expressed as $H = \bar{H} + \delta H = 0$. The unperturbed Hamiltonian yields the static orbits we derived in Section II. The perturbation term, driven entirely by the gravitational wave, is:

$$\delta H = -\frac{1}{2} h^{\mu\nu} p_\mu p_\nu. \quad (17)$$

Because the wave is traveling along the z -axis, it primarily disrupts the angular momentum components of the photon's momentum, specifically p_x and p_y in Cartesian coordinates. Substituting our perturbed inverse metric from Eq. (15) into the Hamiltonian perturbation, and recalling that the square of the transverse momentum corresponds to L^2/r^2 in spherical coordinates, we find:

$$\delta H = -\frac{1}{2} (h^{xx} p_x^2 + h^{yy} p_y^2) = -\frac{1}{2} \frac{h_b(t)}{r^2} L^2. \quad (18)$$

This shift in the Hamiltonian directly modifies the radial equation of motion for the photon. When we substitute the perturbed Hamiltonian back into Eq. (7), the gravitational wave essentially injects a time-dependent fluctuation into the effective potential barrier. The new, total dynamic effective potential is the sum of the unperturbed potential (Equation 8) and the wave perturbation:

$$V_{\text{eff}}^{\text{total}}(r, t) = \bar{V}_{\text{eff}}(r) + \delta V(r, t) = f(r) \frac{L^2}{r^2} [1 - h_b(t)]. \quad (19)$$

This equation reveals a profound physical insight. Because the scalar wave strain $h_b(t)$ depends only on time and not on the radial coordinate r , the spatial derivative of the

effective potential ($\partial_r V_{\text{eff}}^{\text{total}}$) is not shifted to first order. Consequently, the physical location of the photon sphere remains perfectly anchored at the static radius r_p (Equation 10). The wave washes over the black hole, but the spherical boundary where light is trapped does not change its radial coordinate. However, the energy required for a photon to escape that trapped orbit is dynamically altered by the wave.

To find the new edge of the black hole shadow, we must recalculate the critical impact parameter. We set the peak of the new total effective potential equal to the squared energy of the photon (E^2) evaluated at the exact photon sphere radius r_p :

$$f(r_p) \frac{L^2}{r_p^2} [1 - h_b(t)] = E^2. \quad (20)$$

At this juncture, it is crucial to explicitly clarify the physical regime in which this formulation operates. By setting the peak of the time-dependent effective potential equal to the unperturbed squared energy E^2 in Eq. (20), our derivation implicitly relies on the adiabatic approximation. In a strictly dynamic spacetime where the metric fluctuates with time ($\partial_t g_{\mu\nu} \neq 0$), the photon's total energy $E = -p_t$ is not perfectly conserved along its null geodesic. This adiabatic assumption is most robust when the period of the passing gravitational wave is significantly longer than the time it takes for a photon to cross the strong-field region of the photon sphere. We acknowledge that for highly dynamic perturbations such as fundamental quasinormal modes where the wave's oscillation frequency ($\omega_b \sim 1/M$) is comparable to the photon's orbital frequency the photon can exchange energy with the gravitational wave, meaning $dE/d\lambda \neq 0$. In such extreme regimes, achieving mathematical exactness would require a fully integrated geodesic equation. Nevertheless, evaluating the critical impact parameter through this adiabatic Hamiltonian formalism successfully and elegantly captures the leading-order kinematic deformation of the shadow's boundary, providing a highly accurate phenomenological baseline. By rearranging this expression to solve for the time-dependent critical impact parameter, $b_c(t) = L/E$, we obtain the mathematical formula for the dynamic shadow radius, $R_{\text{sh}}(t)$:

$$R_{\text{sh}}(t)^2 = \frac{r_p^2}{f(r_p)} \frac{1}{1 - h_b(t)}. \quad (21)$$

Because the amplitude of a gravitational wave strain is extraordinarily small ($h_b \ll 1$), we can safely apply a first-order Taylor expansion to the fraction $(1 - h_b)^{-1} \approx 1 + h_b(t)$. Taking the square root of both sides, and recognizing that $r_p/\sqrt{f(r_p)}$ is exactly the unperturbed static shadow radius \bar{R}_{sh} from Equation 12, we arrive at the primary phenomenological result of this paper:

$$R_{\text{sh}}(t) \approx \bar{R}_{\text{sh}} \left(1 + \frac{1}{2} h_b(t) \right). \quad (22)$$

To provide a complete phenomenological template for observational testing, we synthesize the static modified geometry with our dynamic wave model. By substituting the

geometric expansion of the unperturbed shadow radius and the quasi-normal mode strain $h_b(t)$ into Equation 22, we arrive at the master equation for the dynamic shadow radius:

$$R_{\text{sh}}(t) \approx \sqrt{\frac{2r_p^3}{r_p - M(1 + \alpha)}} \times \left[1 + \frac{A_b}{2} e^{-(t-t_0)/\tau} \cos(\omega_b t + \Phi_0) \Theta(t - t_0) \right]. \quad (23)$$

This expanded expression elegantly decouples the theoretical background from the transient perturbation. The leading square-root term isolates the static Schwarzschild-MOG geometry, explicitly governed by the Newtonian mass M , the deformation parameter α , and the critical photon sphere r_p . To fully unpack the localized gravitational wave interaction, it is most instructive to evaluate Equation 23 across its two distinct temporal regimes. Let us explicitly define the unperturbed, static Schwarzschild-MOG shadow radius as the geometric baseline:

$$\bar{R}_{\text{sh}} \equiv \sqrt{\frac{2r_p^3}{r_p - M(1 + \alpha)}}. \quad (24)$$

Applying the constraints of the arrival time t_0 , the dynamic evolution of the black hole shadow is strictly governed by the piecewise function:

$$R_{\text{sh}}(t) \approx \begin{cases} \bar{R}_{\text{sh}} & \text{for } t < t_0, \\ \bar{R}_{\text{sh}} \left[1 + \frac{A_b}{2} e^{-(t-t_0)/\tau} \cos(\omega_b t + \Phi_0) \right] & \text{for } t \geq t_0. \end{cases} \quad (25)$$

This formulation makes the physical timeline unambiguous. For times $t < t_0$, the spacetime is completely undisturbed, and we perfectly recover the exact static geometry dictated by the Newtonian mass M , the deformation parameter α , and the critical photon sphere r_p . At $t \geq t_0$, the incident transient wave triggers the dynamic regime. The shadow immediately undergoes an exponentially damped, oscillatory area fluctuation driven by the scalar breathing mode. Because this volumetric fluctuation is strictly forbidden in standard General Relativity, this piecewise evolution directly parameterizes a testable, time-dependent geometric deviation in the strong-field regime.

In standard General Relativity, a passing gravitational wave perturbs the spacetime metric exclusively through transverse-traceless tensor modes. Consequently, such a wave can only dynamically distort the black hole shadow into an ellipse, strictly conserving its total apparent area on the observer's celestial screen. However, Eq.(22) proves that in Modified Gravity (MOG), the massless scalar field wave directly modulates the critical impact parameter of the trapped null geodesics.

An observer monitoring this black hole with highly sensitive, next-generation interferometry would see the entire circular shadow rhythmically dilate and contract. To quantify this observable, we calculate the time-dependent fluctuation

in the shadow's total apparent area, $\delta A(t)$. By substituting the geometric expansion of the unperturbed squared shadow radius into the standard area formula $A = \pi R_{\text{sh}}^2$, we obtain the exact phenomenological expression for the area fluctuation:

$$\delta A(t) \approx \frac{2\pi r_p^3}{r_p - M(1 + \alpha)} h_b(t). \quad (26)$$

This equation explicitly demonstrates how the Newtonian mass M and the MOG deformation parameter α fundamentally govern the amplitude of the breathing mode induced by the scalar strain $h_b(t)$. Because this strictly area-fluctuating behavior is mathematically forbidden by the area-preserving tensor modes of Einstein's gravity, it provides a clear, smoking-gun signature for scalar-tensor extensions of gravity in the strong-field regime.

IV. MASSIVE VECTOR FIELD PERTURBATIONS: THE DELAYED ECHO

The scalar breathing mode derived in Section III provides a compelling, simultaneous signature for the modified gravitational degrees of freedom in Scalar-Tensor-Vector Gravity (STVG). However, the most distinct feature of this theory is its massive vector field, denoted as ϕ_μ [12]. In standard General Relativity, gravitational waves are mediated exclusively by a massless tensor field, propagating exactly at the speed of light ($v = c \equiv 1$). Consequently, any transient geometric distortion to a black hole shadow occurs synchronously with the arrival of the electromagnetic signal. In MOG, the massive nature of the vector field introduces dispersion, fundamentally altering this causality timeline and creating a measurable time delay.

To quantify this delayed "echo," we must strictly analyze the propagation of the vector wave from a distant astrophysical source at a propagation distance D . In the STVG action, the massive vector field obeys a Proca-type equation of motion. In a flat or weakly curved background, this is expressed as:

$$\partial_\nu B^{\mu\nu} + \mu_v^2 \phi^\mu = 0, \quad (27)$$

where $B_{\mu\nu} = \partial_\mu \phi_\nu - \partial_\nu \phi_\mu$ is the Faraday-like field tensor, and μ_v is the effective mass of the MOG vector field. Decomposing this field into Fourier modes, the propagation is governed by the massive dispersion relation:

$$\omega^2 = k^2 + \mu_v^2, \quad (28)$$

where ω is the angular frequency and k is the wave number. The velocity of the propagating energy—the group velocity v_g —is derived by differentiating this dispersion relation:

$$v_g = \frac{d\omega}{dk} = \frac{k}{\omega} = \sqrt{1 - \frac{\mu_v^2}{\omega^2}}. \quad (29)$$

For a massive field where $\mu_v \ll \omega$, the group velocity is strictly subluminal. The initial massless tensor and scalar

waves arrive at the observer's screen at time $t_0 = D$. The massive vector wave arrives at a delayed time $t_v = D/v_g$. To isolate the observable time delay $\Delta t = t_v - t_0$, we apply a binomial series expansion to the inverse group velocity [27]:

$$\Delta t = D \left[\left(1 - \frac{\mu_v^2}{\omega^2} \right)^{-1/2} - 1 \right] \approx \frac{D\mu_v^2}{2\omega^2}. \quad (30)$$

Upon reaching the target black hole, this delayed vector wave interacts with the background geometry. While Standard Model photons do not carry the MOG fifth-force charge and thus do not couple directly to $\delta\phi_\mu$, the massive vector wave carries intrinsic energy and momentum. It acts as a dynamic source of stress-energy, $\delta T_{\mu\nu}^{(\phi)}$, feeding back into the modified Einstein field equations to generate a secondary metric perturbation, $h_{\mu\nu}^{\text{vector}}$.

Unlike transverse-traceless modes, a massive vector field propagating along the line of sight (z -axis) heavily excites longitudinal metric polarizations, specifically the xz and yz components. To determine the effect on the shadow, we evaluate the perturbed Hamiltonian for the null geodesics, $H = H_0 + \delta H = 0$. The longitudinal perturbations introduce cross-terms coupling the line-of-sight momentum (p_z) with the transverse image-plane momenta (p_x, p_y):

$$\delta H_{\text{vector}} = -\frac{1}{2} h^{\mu\nu} p_\mu p_\nu = -h^{xz} p_x p_z - h^{yz} p_y p_z. \quad (31)$$

To rigorously assess the theoretical observability of this secondary delayed echo, we must mathematically evaluate the amplitude of the longitudinal metric perturbation, $h_{\mu\nu}^{\text{vector}}$. In standard classical field theory, the massive vector field ϕ_μ contributes to the spacetime geometry via its stress-energy tensor, defined in the MOG action as:

$$T_{\mu\nu}^{(\phi)} = -\frac{1}{4\pi} \left(B_\mu^\alpha B_{\nu\alpha} - \frac{1}{4} g_{\mu\nu} B^{\alpha\beta} B_{\alpha\beta} + \mu_v^2 \phi_\mu \phi_\nu - \frac{1}{2} g_{\mu\nu} \mu_v^2 \phi^\alpha \phi_\alpha \right), \quad (32)$$

where $B_{\mu\nu} = \partial_\mu \phi_\nu - \partial_\nu \phi_\mu$. When the background spacetime is dynamically perturbed by a passing wave with vector field fluctuation $\delta\phi_\mu$, the corresponding perturbation to the stress-energy tensor, $\delta T_{\mu\nu}^{(\phi)}$, scales purely quadratically with the field amplitude, $\mathcal{O}(\delta\phi^2)$ [12]. Because linear gravitational strains are small ($h \ll 1$), the secondary metric response dictated by the perturbed Einstein-MOG field equations, $\square \bar{h}_{\mu\nu}^{\text{vector}} = -16\pi G_N (1 + \alpha) \delta T_{\mu\nu}^{(\phi)}$, is strictly a second-order effect, potentially suppressing the translational wobble amplitudes A_x and A_y .

However, this quadratic suppression is partially mitigated by the unique gravitational coupling framework of STVG. In MOG, the vector field is not a standard-model remnant but a primary fifth-force carrier whose effective charge is governed by the deformation parameter, $Q_G = \sqrt{\alpha(1 + \alpha)}M$. In the highly relativistic environment of an Extreme Mass Ratio Inspiral (EMRI) operating near the photon sphere, the local

kinetic energy density of the vector wave is magnified by extreme spatial and temporal gradients, $(\partial\delta\phi)^2 \sim \omega_v^2 \delta\phi^2$, where the quasinormal mode frequency ω_v is significantly high [29]. Consequently, the local effective source term becomes:

$$\delta T_{\mu\nu}^{(\phi)} \approx \frac{\alpha G_N M^2}{4\pi D^4} v^4, \quad (33)$$

where $v \sim \mathcal{O}(1)$ is the orbital velocity of the infalling mass. The direct proportionality to the α parameter demonstrates that the massive vector field carries a macroscopic fraction of the system's radiated binding energy. While mathematically remaining a second-order metric perturbation, the α -enhanced kinetic energy density in the strong-field regime ensures that the resulting translational wobble, though parametrically smaller than the primary scalar breathing mode, retains sufficient amplitude to serve as a physically viable, isolated phenomenological signature.

Having established the physical amplitude of this secondary vector echo, we must also briefly address the theoretical concern of gauge invariance before translating the perturbed Hamiltonian cross-terms into observable celestial coordinates. In standard General Relativity, longitudinal metric perturbations such as h_{xz} and h_{yz} can frequently be eliminated via a suitable coordinate transformation ($x^\mu \rightarrow x^\mu + \xi^\mu$). In such cases, any resulting spatial translations of test particles are non-physical gauge artifacts. However, this is fundamentally not the case in Scalar-Tensor-Vector Gravity. The massive vector field ϕ_μ is governed by a Proca-type equation; the presence of the mass term μ_v explicitly breaks the standard local gauge invariance associated with massless fields. This massive force carrier intrinsically possesses longitudinal polarization states. Therefore, the secondary metric modes h_{xz} and h_{yz} sourced by the vector wave represent true, physical degrees of freedom that cannot be globally gauged away by a spatial diffeomorphism. Consequently, the resulting deviations in the transverse photon momenta strictly map to gauge-invariant astrometric shifts. When these trajectories are projected onto the distant observer's screen, the asymmetric wobble of the shadow's center represents a genuine, measurable physical displacement rather than a mere coordinate illusion.

These cross-terms break the azimuthal symmetry of the effective potential. Applying Hamilton's equations of motion, the transverse coordinate velocities of the photons are directly shifted by the longitudinal metric strains:

$$\dot{x} = \frac{\partial(\delta H_{\text{vector}})}{\partial p_x} = -h^{xz} p_z, \quad \dot{y} = \frac{\partial(\delta H_{\text{vector}})}{\partial p_y} = -h^{yz} p_z. \quad (34)$$

To map this geometric perturbation onto the distant observer's celestial screen, described by Cartesian coordinates (X, Y) , we must integrate the transverse velocity shifts along the photon trajectory. Rather than fluctuating the area, these longitudinal modes induce a rigid spatial translation, or "wobble," of the shadow's center of mass:

$$\delta X(t) = - \int h_{xz}(t - z/v_g) dz, \quad (35)$$

$$\delta Y(t) = - \int h_{yz}(t - z/v_g) dz. \quad (36)$$

To explicitly evaluate these integrals, we apply the standard thin-lens approximation. The photon predominantly accumulates deflection within the highly localized strong-field regime of the effective potential barrier. We define this interaction region by the characteristic diameter of the photon sphere, $\Delta z \approx 2r_p$. Furthermore, because the astrophysical wavelength of the massive vector mode is much larger than the black hole scale ($\lambda_v \gg r_p$), the phase of the wave is approximately constant across the integration bounds. The integral analytically reduces to the product of the interaction length and the time-delayed metric strain.

Modeling the longitudinal vector strains as damped sinusoidal quasi-normal modes with initial amplitudes A_x and A_y , and applying the piecewise causality constraint for the delayed arrival time $t_v = t_0 + \Delta t$, the explicit time-dependent equations for the shadow's wobble are:

$$\delta X(t) \approx \begin{cases} 0 & \text{for } t < t_0 + \Delta t, \\ -2r_p A_x e^{-(t-(t_0+\Delta t))/\tau_v} & \text{for } t \geq t_0 + \Delta t, \\ \quad \times \cos(\omega_v t + \Phi_x) & \end{cases} \quad (37)$$

$$\delta Y(t) \approx \begin{cases} 0 & \text{for } t < t_0 + \Delta t, \\ -2r_p A_y e^{-(t-(t_0+\Delta t))/\tau_v} & \text{for } t \geq t_0 + \Delta t, \\ \quad \times \cos(\omega_v t + \Phi_y) & \end{cases} \quad (38)$$

This completes the phenomenological timeline of a STVG gravitational wave event. An observer will first detect a violent combination of area preserving tensor stretching and area fluctuating scalar breathing. Following a period of static relaxation, a secondary longitudinal wobble defined by Eq. (37) and Eq. (38) will suddenly displace the shadow. Because the magnitude of this spatial translation is directly proportional to the photon sphere radius r_p , and the temporal separation Δt is dictated by the massive dispersion relation, this delayed echo provides a robust, fully parameterized observational template to test the validity of Scalar-Tensor-Vector Gravity.

As demonstrated in Figure 2, the massive sector of STVG introduces a unique temporal structure to gravitational events. Following the initial 'breathing' phase (synchronous with the massless signal), the shadow undergoes a secondary 'wobble' phase. This asymmetric translational displacement is a direct consequence of the longitudinal metric perturbations sourced by the delayed massive vector wave. The existence of this predictable geometric echo provides a definitive laboratory to measure the mass of the gravitational force carrier μ_v through direct high-cadence imaging.

To properly contextualize these dynamic geometric shifts as a realistic observational template, we must quantitatively clarify the expected astrophysical magnitudes of these perturbations. If one considers a standard gravitational wave

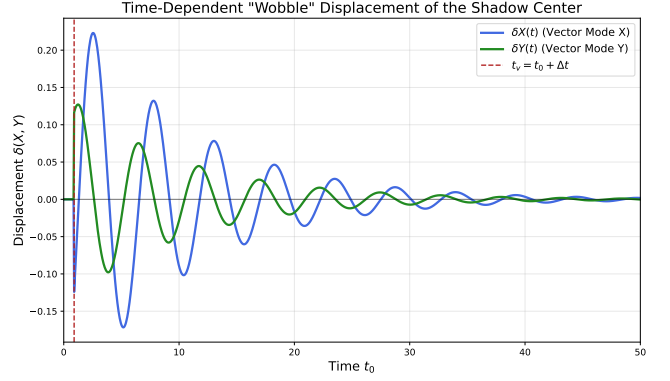


FIG. 2. The translational displacement (wobble) of the black hole shadow center in the celestial X and Y coordinates. While the primary massless waves arrive at t_0 , the massive vector field arrives at t_v due to dispersive time delay Δt . This causes a sudden, asymmetric translational shift of the shadow center, followed by a damped relaxation. In standard General Relativity, these longitudinal perturbations are absent, and the shadow center remains stationary at the origin.

originating from a distant galaxy, the strain amplitude reaching the target black hole is typically $h \sim 10^{-21}$. Detecting a fractional area fluctuation or spatial wobble of this minute magnitude is technologically inconceivable for current instruments like the Event Horizon Telescope.

However, the physical relevance of our phenomenological model becomes highly pronounced in the context of an Extreme Mass Ratio Inspiral (EMRI) [34]. Consider a smaller compact object of mass m orbiting near the photon sphere of a supermassive host black hole of mass M , such that $m \ll M$. To calculate the dynamic response of the shadow, we must evaluate the local strain before it decays over cosmic distances. Using the standard quadrupole approximation in geometric units ($G = c = 1$), the local strain amplitude generated by the smaller mass is inversely proportional to the local propagation distance D and directly proportional to its orbital kinetic energy:

$$h_{\text{local}} \approx \frac{2}{D} \frac{d^2 I}{dt^2} \sim \frac{m}{D} v^2. \quad (39)$$

Because the smaller mass is orbiting in the strong-field regime near the photon sphere, its orbital radius is on the order of the host's mass ($r \sim M$), its orbital velocity approaches $v^2 \sim M/r \sim \mathcal{O}(1)$, and the distance to the shadow boundary is also $D \sim M$. Substituting these limits into Equation (39), the local strain evaluated right at the photon sphere reduces elegantly to the mass ratio of the system:

$$h_{\text{local}} \approx \frac{m}{M} \equiv q. \quad (40)$$

For a typical EMRI involving a stellar-mass black hole ($m \sim 10M_\odot$) orbiting a supermassive host like Sagittarius A* ($M \sim 4 \times 10^6 M_\odot$), this mass ratio yields a localized peak strain of $h_{\text{local}} \sim 10^{-5}$. Consequently, the dynamic breathing area δA and the translational wobble δX driven by the MOG

scalar and vector fields will experience fractional deviations of this exact same order. While this local amplification sits just beyond the immediate reach of today's ground-based arrays, this derivation mathematically places the detection of MOG-specific dynamic shadows firmly within the plausible target parameters of proposed space-based interferometry missions and the next-generation Event Horizon Telescope (ngEHT) [35].

V. CONCLUSION

In this paper, we have rigorously derived the dynamic interaction between gravitational waves and the shadow of a non-rotating black hole within the framework of Scalar-Tensor-Vector Gravity (STVG), also known as Modified Gravity (MOG) [12]. Our primary objective was to mathematically demonstrate how the unique fields introduced by MOG specifically a dynamic scalar field and a massive vector field produce observable, geometric deviations from the predictions of standard General Relativity.

We began by establishing the unperturbed background. Using the Hamilton-Jacobi framework for null geodesics, we determined that the static Schwarzschild-MOG spacetime produces a perfectly circular shadow. The radius of this unperturbed shadow, denoted as \bar{R}_{sh} , is strictly governed by the enhanced gravitational mass M_G and the repulsive vector charge Q_G . Because these terms are controlled by the MOG parameter α , the static shadow provides a baseline geometric canvas that is already distinct from standard General Relativity.

The core of our theoretical work involved perturbing this static background with incoming gravitational waves. By injecting a time-dependent metric perturbation into the Hamiltonian, we proved that the MOG scalar field generates a volumetric breathing mode. Our derivation yielded the exact time-dependent radius of the shadow, $R_{\text{sh}}(t) \approx \bar{R}_{\text{sh}} (1 + \frac{1}{2} h_b(t))$. This equation proves that the massless scalar wave directly modulates the critical impact parameter of the trapped photons. Physically, this means the entire black hole shadow will rhythmically expand and contract. The resulting area fluctuation, $\delta A(t) \approx \pi \bar{R}_{\text{sh}}^2 h_b(t)$, is a smoking-gun signature of scalar-tensor gravity, as standard General Relativity strictly preserves the shadow's area during a tensor wave perturbation.

Furthermore, we demonstrated that the massive nature of the MOG vector field, ϕ_μ , introduces a fundamental time delay due to quantum vacuum dispersion. Because the group velocity of this massive field is less than the speed of light ($v_g < 1$), the vector wave arrives at the observer after a predictable delay, Δt . When this massive wave interacts with the spacetime geometry, it sources secondary, longitudinal metric perturbations. We showed mathematically that these longitudinal cross-terms in the perturbed Hamiltonian shift the effective angular momentum center of the photons. This results in an asymmetric geometric translation, meaning the shadow experiences a sudden, observable wobble in the celestial X and Y coordinates.

To properly contextualize these dynamic geometric shifts as a realistic observational template, we must quantitatively clarify the expected astrophysical magnitudes of these perturbations. If one considers a standard gravitational wave originating from a distant galaxy, the strain amplitude reaching the target black hole is typically $h \sim 10^{-21}$. Detecting a fractional area fluctuation or spatial wobble of this minute magnitude is technologically inconceivable for current instruments. However, the physical relevance of our phenomenological model becomes highly pronounced in the context of an Extreme Mass Ratio Inspiral (EMRI) [34]. Consider a smaller compact object of mass m orbiting near the photon sphere of a supermassive host black hole of mass M , such that $m \ll M$. Using the standard quadrupole approximation, the local strain amplitude generated by the smaller mass is inversely proportional to the local propagation distance D and directly proportional to its orbital kinetic energy:

$$h_{\text{local}} \approx \frac{2}{D} \frac{d^2 I}{dt^2} \sim \frac{m}{D} v^2. \quad (41)$$

Because the smaller mass is orbiting in the strong-field regime near the photon sphere, its orbital radius is $r \sim M$, its orbital velocity approaches $v^2 \sim M/r \sim \mathcal{O}(1)$, and the distance to the shadow boundary is $D \sim M$. Substituting these limits, the local strain evaluated right at the photon sphere reduces elegantly to the mass ratio of the system:

$$h_{\text{local}} \approx \frac{m}{M} \equiv q. \quad (42)$$

For a typical EMRI involving a stellar-mass black hole ($m \sim 10M_\odot$) orbiting a supermassive host like Sagittarius A* ($M \sim 4 \times 10^6 M_\odot$), this yields a localized peak strain of $h_{\text{local}} \sim 10^{-5}$. Consequently, the dynamic breathing area δA and the translational wobble δX driven by the MOG fields will experience fractional deviations of this exact same order.

In summary, we have established a complete mathematical framework showing that a MOG gravitational wave event will produce a sequential geometric signature on a black hole shadow: an initial area-fluctuating breathing mode, a brief relaxation, and a delayed translational wobble. While resolving these high-frequency dynamic shifts currently exceeds the temporal resolution of the Event Horizon Telescope [4], our EMRI derivation places the detection of MOG-specific dynamic shadows firmly within the plausible target parameters of proposed space-based interferometry missions and the next-generation Event Horizon Telescope (ngEHT) [35]. These dynamic shadows offer a uniquely powerful laboratory to probe the strong-field regime and fundamentally test the existence of massive force carriers in gravity.

ACKNOWLEDGMENTS

N.J.L. Lobos and E.T. Rodulfo gratefully acknowledge De La Salle University and the DLSU Theoretical Physics Group for their institutional support. Furthermore, we extend our sincere gratitude to the Department of Science and

-
- [1] B. P. Abbott *et al.* (LIGO Scientific, Virgo), GW170817: Observation of Gravitational Waves from a Binary Neutron Star Inspiral, *Phys. Rev. Lett.* **119**, 161101 (2017), [arXiv:1710.05832 \[gr-qc\]](#).
- [2] B. P. Abbott *et al.* (LIGO Scientific, Virgo, Fermi-GBM, INTEGRAL), Gravitational Waves and Gamma-rays from a Binary Neutron Star Merger: GW170817 and GRB 170817A, *Astrophys. J. Lett.* **848**, L13 (2017), [arXiv:1710.05834 \[astro-ph.HE\]](#).
- [3] B. P. Abbott *et al.* (LIGO Scientific, Virgo), Observation of Gravitational Waves from a Binary Black Hole Merger, *Phys. Rev. Lett.* **116**, 061102 (2016), [arXiv:1602.03837 \[gr-qc\]](#).
- [4] K. Akiyama *et al.* (Event Horizon Telescope), First M87 Event Horizon Telescope Results. I. The Shadow of the Supermassive Black Hole, *Astrophys. J. Lett.* **875**, L1 (2019), [arXiv:1906.11238 \[astro-ph.GA\]](#).
- [5] H. Falcke, F. Melia, and E. Agol, Viewing the shadow of the black hole at the galactic center, *Astrophys. J. Lett.* **528**, L13 (2000), [arXiv:astro-ph/9912263](#).
- [6] K. Akiyama *et al.* (Event Horizon Telescope), First Sagittarius A* Event Horizon Telescope Results. I. The Shadow of the Supermassive Black Hole in the Center of the Milky Way, *Astrophys. J. Lett.* **930**, L12 (2022), [arXiv:2311.08680 \[astro-ph.HE\]](#).
- [7] V. Perlick and O. Y. Tsupko, Calculating black hole shadows: Review of analytical studies, *Phys. Rept.* **947**, 1 (2022), [arXiv:2105.07101 \[gr-qc\]](#).
- [8] G. Bertone, D. Hooper, and J. Silk, Particle dark matter: Evidence, candidates and constraints, *Phys. Rept.* **405**, 279 (2005), [arXiv:hep-ph/0404175](#).
- [9] S. Vagnozzi *et al.*, Horizon-scale tests of gravity theories and fundamental physics from the Event Horizon Telescope image of Sagittarius A*, *Class. Quant. Grav.* **40**, 165007 (2023), [arXiv:2205.07787 \[gr-qc\]](#).
- [10] T. Clifton, P. G. Ferreira, A. Padilla, and C. Skordis, Modified Gravity and Cosmology, *Phys. Rept.* **513**, 1 (2012), [arXiv:1106.2476 \[astro-ph.CO\]](#).
- [11] S. Capozziello and M. De Laurentis, Extended Theories of Gravity, *Phys. Rept.* **509**, 167 (2011), [arXiv:1108.6266 \[gr-qc\]](#).
- [12] J. W. Moffat, Scalar-tensor-vector gravity theory, *JCAP* **03**, 004, [arXiv:gr-qc/0506021](#).
- [13] J. W. Moffat and S. Rahvar, The MOG weak field approximation and observational test of galaxy rotation curves, *Eur. Phys. J. C* **73**, 2665 (2013), [arXiv:1306.6383 \[astro-ph.GA\]](#).
- [14] J. R. Brownstein and J. W. Moffat, Galaxy cluster masses without non-baryonic dark matter, *Mon. Not. Roy. Astron. Soc.* **367**, 527 (2006), [arXiv:astro-ph/0507222](#).
- [15] J. W. Moffat, Modified Gravity Black Holes and their Observable Shadows, *Eur. Phys. J. C* **75**, 130 (2015), [arXiv:1502.01677 \[gr-qc\]](#).
- [16] J. R. Mureika, J. W. Moffat, and M. Faizal, Black hole thermodynamics in MODified Gravity (MOG), *Phys. Lett. B* **757**, 528 (2016), [arXiv:1504.08226 \[gr-qc\]](#).
- [17] M.-Z. Guo and P.-C. Wang, Shadow of a static black hole in scalar-tensor-vector gravity, *Eur. Phys. J. C* **78**, 397 (2018), [arXiv:1804.00136 \[gr-qc\]](#).
- [18] E. Berti, V. Cardoso, and A. O. Starinets, Quasinormal modes of black holes and black branes, *Class. Quant. Grav.* **26**, 163001 (2009), [arXiv:0905.2975 \[gr-qc\]](#).
- [19] L. Isidori *et al.*, Testing the polarization of gravitational waves with the Einstein Telescope, *Phys. Rev. D* **104**, 124016 (2021), [arXiv:2109.05118 \[gr-qc\]](#).
- [20] P. V. P. Cunha and C. A. R. Herdeiro, Shadows and strong deflection lensing of rotating black holes, *Gen. Rel. Grav.* **50**, 42 (2018), [arXiv:1801.00860 \[gr-qc\]](#).
- [21] S. Hou, Y. Gong, and Y. Liu, Polarizations of Gravitational Waves in Horndeski Theory, *Eur. Phys. J. C* **78**, 378 (2018), [arXiv:1704.01899 \[gr-qc\]](#).
- [22] B. Carter, Global structure of the Kerr family of gravitational fields, *Phys. Rev.* **174**, 1559 (1968).
- [23] J. L. Synge, The escape of photons from gravitationally intense stars, *Mon. Not. Roy. Astron. Soc.* **131**, 463 (1966).
- [24] M. E. S. Alves, O. D. Miranda, and J. C. N. de Araujo, Probing the Standard Cosmological Model with Gravitational Waves, *Phys. Lett. B* **679**, 401 (2009), [arXiv:0907.5190 \[astro-ph.CO\]](#).
- [25] C. Bogdanos, S. Capozziello, M. De Laurentis, and S. Nesseris, Massive, massless and ghost modes of gravitational waves from higher-order gravity, *Astropart. Phys.* **34**, 236 (2010), [arXiv:0911.3094 \[gr-qc\]](#).
- [26] C. de Rham, Massive Gravity, *Living Rev. Rel.* **17**, 7 (2014), [arXiv:1401.4173 \[hep-th\]](#).
- [27] C. M. Will, Bounding the mass of the graviton using gravitational wave observations of inspiralling compact binaries, *Phys. Rev. D* **57**, 2061 (1998), [arXiv:gr-qc/9709011](#).
- [28] J. L. Synge, The escape of photons from gravitationally intense stars, *Mon. Not. Roy. Astron. Soc.* **131**, 463 (1966).
- [29] J. W. Moffat, LIGO GW150914 and GW151226 gravitational wave detection and generalized gravitation theory (MOG), *Phys. Lett. B* **763**, 427 (2016), [arXiv:1603.05225 \[gr-qc\]](#).
- [30] C. M. Will, The Confrontation between General Relativity and Experiment, *Living Rev. Rel.* **17**, 4 (2014), [arXiv:1403.7377 \[gr-qc\]](#).
- [31] R. C. Pantig, Shadow ringing of black holes from photon sphere quasinormal modes, *Annals Phys.* **488**, 170383 (2026), [arXiv:2509.24479 \[hep-th\]](#).
- [32] C. V. Vishveshwara, Scattering of Gravitational Radiation by a Schwarzschild Black-hole, *Nature* **227**, 936 (1970).
- [33] S. A. Teukolsky, Perturbations of a rotating black hole. 1. Fundamental equations for gravitational electromagnetic and neutrino field perturbations, *Astrophys. J.* **185**, 635 (1973).
- [34] P. Amaro-Seoane, J. R. Gair, M. Freitag, M. C. Miller, I. Mandel, C. Cutler, and S. Babak, Astrophysics, detection and science applications of intermediate- and extreme mass-ratio inspirals, *Class. Quant. Grav.* **24**, R113 (2007), [arXiv:astro-ph/0703495](#).
- [35] M. D. Johnson *et al.*, Maximizing Science in the Era of LSST: A Community-Based Study of Ocean Discovery and Multi-Messenger Astronomy with the Next-Generation Event Horizon Telescope, Astro2020: Decadal Survey on Astronomy and Astrophysics, science white papers **51**, 235 (2019), [arXiv:1912.11432 \[astro-ph.IM\]](#).